Implications for first-order cosmological phase transitions and the formation of primordial black holes from the third LIGO-Virgo observing run

Alba Romero-Rodríguez, Katarina Martinovic, Thomas A. Callister, Huai-Ke Guo, Mario Martínez, Oriol Pujolàs, Mairi Sakellariadou, Ville Vaskonen, Feng-Wei Yang and Yue Zhao

EPS-HEP 2021, July 26-30 2021

Motivation

- Apart from detecting gravitational waves (GWs) from compact binary coalescences (CBCs), Advanced LIGO and Advance Virgo can probe stochastic gravitational wave backgrounds (SGWB), providing information about the early Universe.
- The SGWB is a superposition of GWs sources [1] that can be:
  - Astrophysical: distant CBCs that cannot be resolved individually, core collapse supernovae, rotating neutron stars and stellar core collapses.
  - Cosmological: cosmic strings, primordial black holes, superradiance of axion clouds around black holes, phase transitions in the early Universe, and GWs produced during or at the end of inflation.

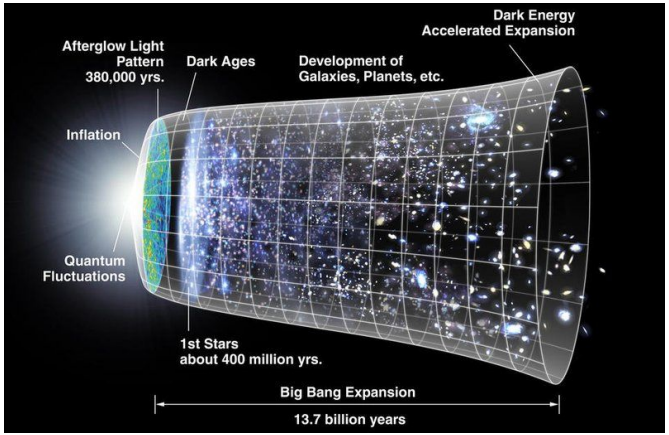

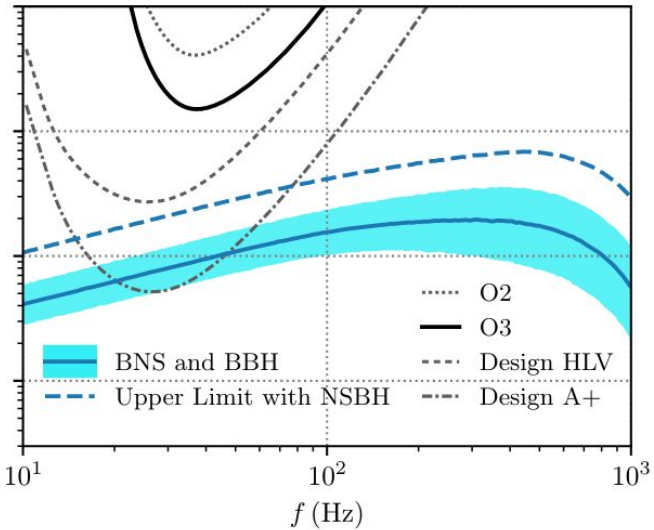

[1]

[1] R. Abbott et al. (LIGO Scientific, Virgo, KAGRA) (2021), 2101.12130.

Motivation

- We focus on two of these sources for the following reasons:
  - Models Beyond the Standard Model (BSM) predict First Order Phase Transitions (FOPTs) in the early Universe. Energies >> energy scale of Big Bang Nucleosynthesis and the CMB (unreachable at LHC). The production of GWs in FOPTs is then an alternative probe.
  - Primordial Black Holes (PBHs) have gained interest as the particle dark matter candidates have become increasingly tightly constrained. Even very light PBHs that have evaporated after formation can have an impact in the formation of dark matter and baryon asymmetry in the Universe.
- The SGWB is described in terms of the energy density in gravitational waves spectrum, which is defined in terms of the critical energy density needed to have a flat Universe $\rho_c = 3H_0^2c^2/(8\pi G)$ and the energy density in gravitational waves ρ_{GW} .

$$\Omega_{\mathrm{GW}}(f) = \frac{f}{\rho_c}\frac{\mathrm{d}\rho_{\mathrm{GW}}}{\mathrm{d}f}$$

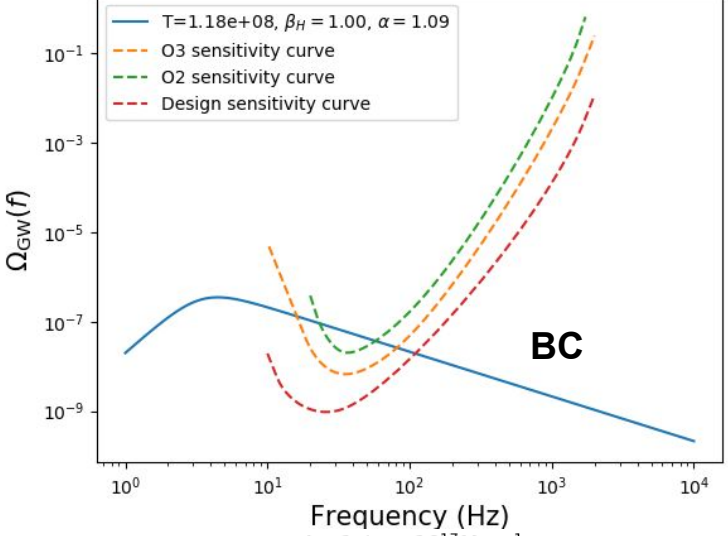

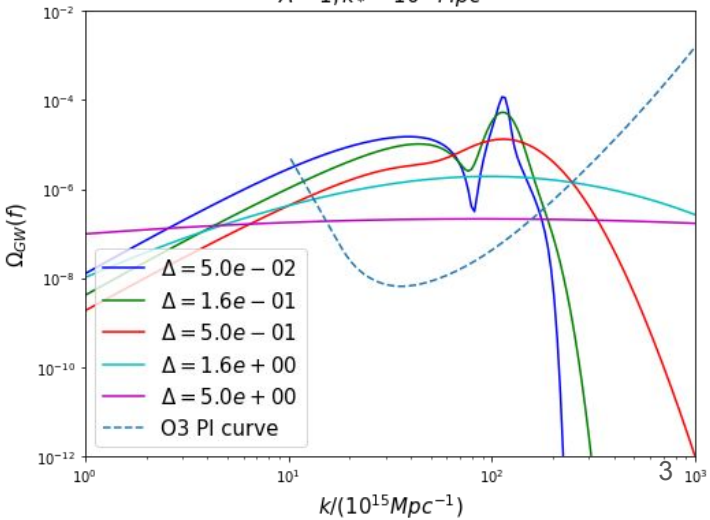

Outline

- In this work we perform a Bayesian search [1,2] in which we assume a SGWB sourced by CBCs and either PBHs or cosmological FOPTs. We neglect the contribution from Schumann resonances, following the reasoning in [3].
- We use O1+O2+O3 correlated data from the three baselines that is already publicly available.
- The results from the isotropic SGWB searches show no evidence for a signal, so we place upper limits (ULs) over the parameters of the energy density spectra.

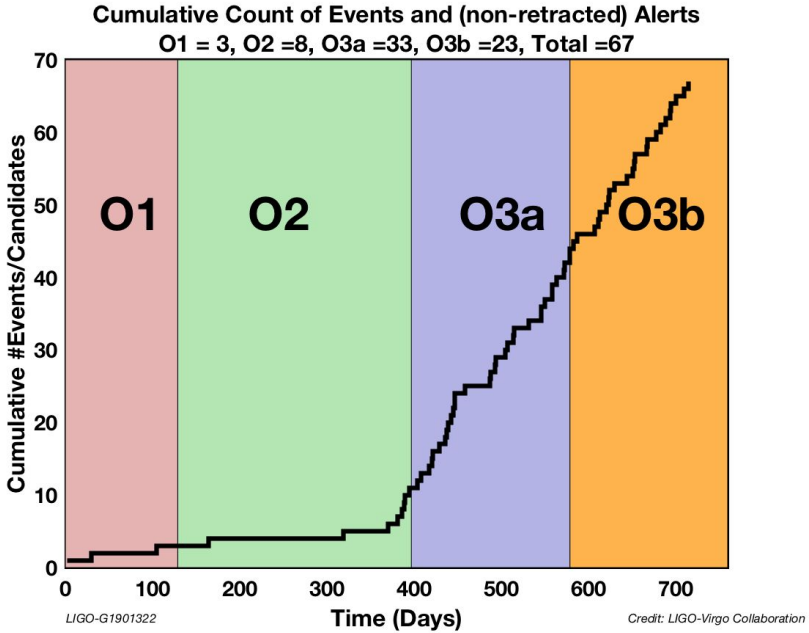

[1] V. Mandic, E. Thrane, S. Giampanis, and T. Regimbau, Phys. Rev. Lett. 109, 171102 (2012), 1209.3847.
[2] P. M. Meyers, K. Martinovic, N. Christensen, and M. Sakellariadou, Phys. Rev. D 102, 102005 (2020), 2008.00789.
[3] A. Romero, K. Martinovic, T. A. Callister, H.-K.Guo, M. Martínez, M. Sakellariadou, F.-W. Yang,and Y. Zhao, Phys. Rev. Lett.126, 151301 (2021), 2102.01714.

Introduction to FOPTs and PBHs, and generation of GWs

- PBHs were formed in the early Universe when large density perturbations collapsed or, said otherwise, when they re-entered the horizon after inflation. At this point is when GWs were generated.
- In a cosmological FOPT the Universe goes from a metastable high energy (symmetric) phase (FV) to a stable lower energy (broken) phase (TV). Process: quantum or thermal nucleation of bubbles of the TV, separated from the surrounding unbroken phase by a wall, which generates GWs.

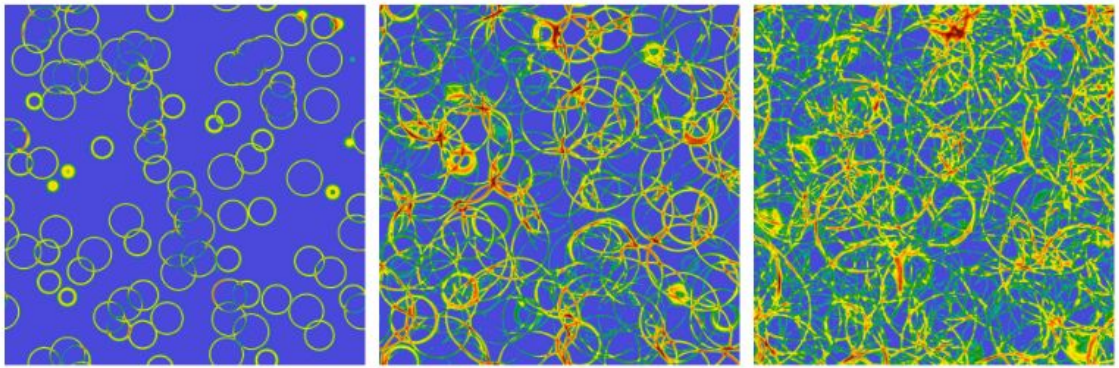

[1]

[1] Mark Hindmarsh, Stephan J. Huber, Kari Rummukainen, and David J. Weir Phys. Rev. D **92**, 123009 (2015).

Multibaseline likelihood

We choose a Gaussian log-likelihood for a single detector pair,

$$\log p(\hat{C}_{IJ}(f)|\boldsymbol{\theta}_{\rm gw}, \lambda) \propto -\frac{1}{2}\sum_f \frac{\left[\hat{C}_{IJ}(f) - \lambda\,\Omega_{\rm gw}(f, \boldsymbol{\theta}_{\rm gw})\right]^2}{\sigma^2_{IJ}(f)},$$

where the data from the O3 analysis is encoded in:

- $\hat{C}_{IJ}(f)$ is the cross-correlation estimator of the SGWB calculated using data from detectors I and J.
- $\sigma^2_{IJ}(f)$ is the corresponding variance.

The GW model we fit to the data is $\Omega_{\rm GW}(f, \boldsymbol{\theta}_{\rm gw})$, with parameters $\boldsymbol{\theta}_{\rm gw}$. λ represents the calibration uncertainties of the detectors.

Model selection and comment on Schumann resonances

We use the Bayes factors (BF) to show preference for one model over another. E.g.

$$\mathcal{B}^{\mathrm{GW}}_{\mathrm{NOISE}} = \frac{\int \mathrm{d}\boldsymbol{\theta}_{\mathrm{gw}}\, p(\hat{C}_{IJ}(f)|\boldsymbol{\theta}_{\mathrm{gw}})p(\boldsymbol{\theta}_{\mathrm{gw}})}{\mathcal{N}},$$

where $\mathcal{N}$ is given by evaluating the log likelihood with $\Omega_{\mathrm{GW}}(f) = 0$, and $p(\boldsymbol{\theta}_{\mathrm{gw}})$ is the prior on the GW model parameters. In the case that $\log \mathcal{B}^{S}_{N} < 0$, there is no evidence for a signal described by the chosen model.

- There is no evidence for correlated magnetic noise in O3. Data is well described by a Gaussian stationary noise model, so we do not fit for Schumann resonances.

FOPTs

Sources of GWs

The TV bubbles expand, collide and eventually coalesce, generating shear stresses which source GWs → three sources of GWs:

- Bubble collisions (BC): $\Omega_{\rm coll}$
- Sound waves (SW): Ω_{sw}. These are the dominant GW production mechanism.
- Turbulence: Ω_t. We will consider it negligible.

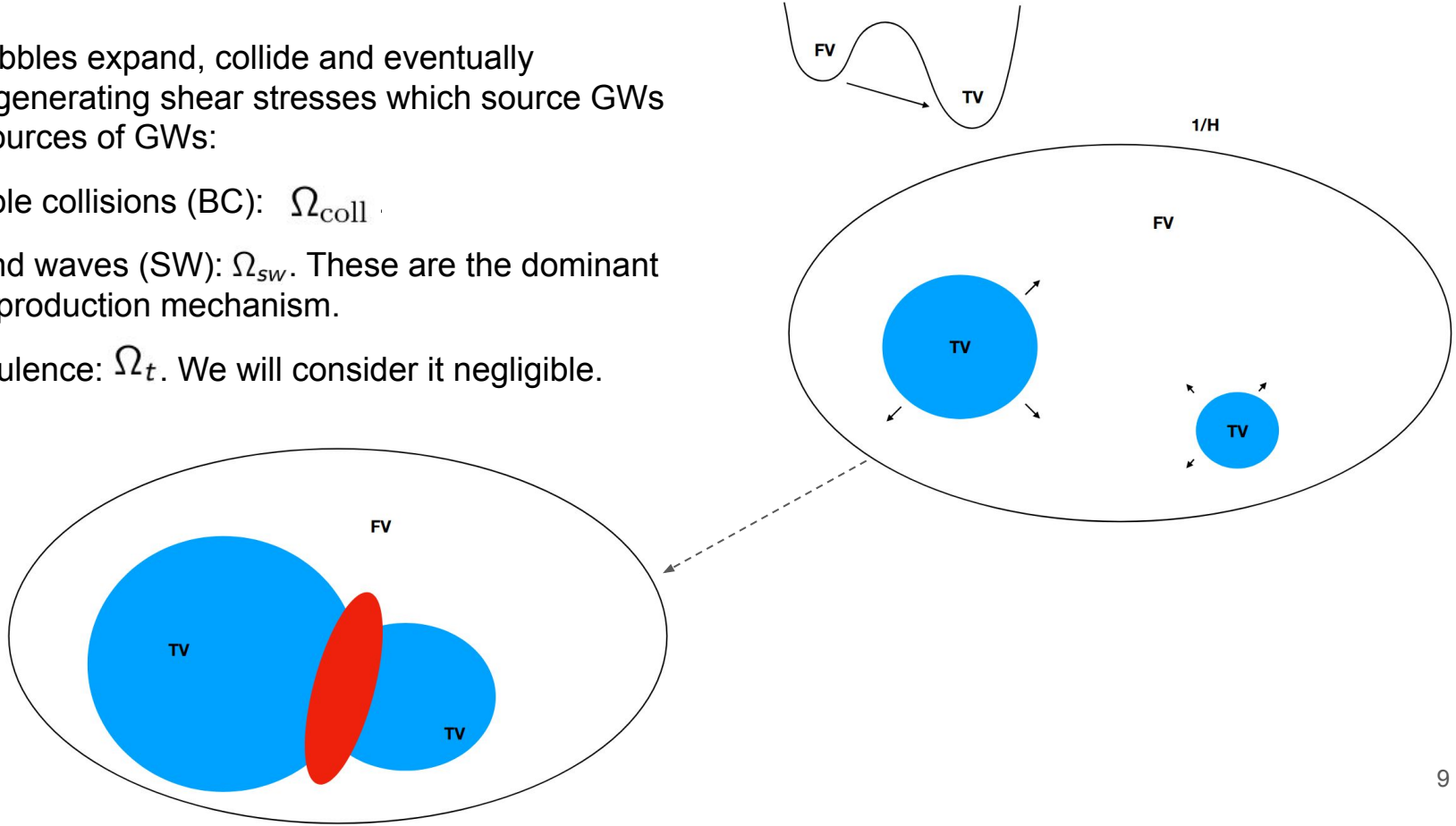

Searches performed

We have performed a series of searches including a CBC background, since it is a non-negligible component of any SGWB signal. We model it as:

$$\Omega_{\mathrm{CBC}} = \Omega_{\mathrm{ref}} \left(\frac{f}{f_{\mathrm{ref}}} \right)^{2/3}, \text{ where } f_{\mathrm{ref}} = 25\mathrm{Hz}$$

We take two different approaches in constraining the SGWB due to FOPTs. Approximated broken power law (BPL)

- BPL
- CBC + BPL

Analytical phenomenological model

- CBC + BC
- CBC + SW

Smooth broken power law

We simplify and model the phase transition contribution as a smooth BPL function,

$$\Omega_{\rm BPL}(f) = \Omega_* \left(\frac{f}{f_*}\right)^{n_1} \left[1 + \left(\frac{f}{f_*}\right)^{\Delta}\right]^{(n_2-n_1)/\Delta}.$$

Where we fix $n_1 = 3$ by causality, $\Delta = 2$ [1], and depending on the source of the GWs, n_2 takes the values:

- $n_2 = -1 \rightarrow$ corresponding to assuming GW sourced by BC
- $n_2 = -4 \rightarrow$ corresponding to assuming GW sourced by SW

With this, we present results for $\Omega_{\rm BPL}$ considering as parameters: $\boldsymbol{\theta}_{\rm gw} = (\Omega_{\rm ref}, f_*, \Omega_*)$.

Priors and results from the CBC+BPL search

$$\Omega_{\rm BPL}(f) = \Omega_* \left(\frac{f}{f_*}\right)^{n_1} \left[1 + \left(\frac{f}{f_*}\right)^{\Delta}\right]^{(n_2-n_1)/\Delta}$$

Broken power law model	
Parameter	Prior
$\Omega_{\rm ref}$	LogUniform(10^{-10}, 10^{-7})
Ω_*	LogUniform(10^{-9}, 10^{-4})
f_*	Uniform(0, 256 Hz)
n_1	3
n_2	Uniform(-8,0)
Δ	2

The narrow, informative prior on $\Omega_{\rm ref}$ stems from the estimate of the CBC background. The peak frequency prior is uniform across the frequency range considered since we have no information about it.

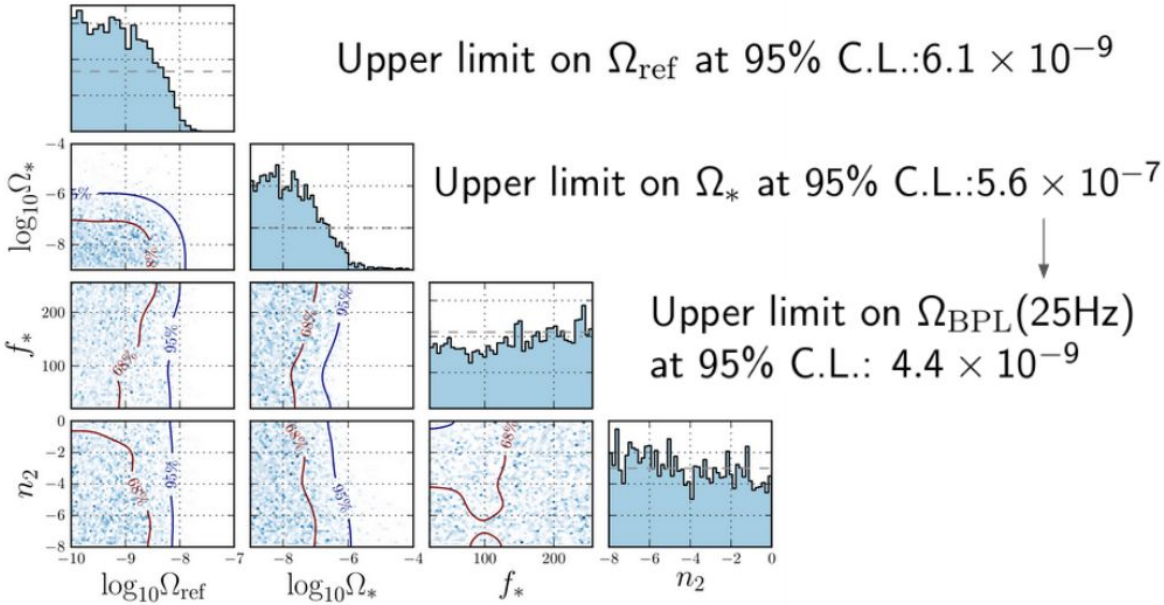

Posterior distributions for the parameters of this model. In all of these searches, the UL at 95% CL on $\Omega_{\rm ref}$ is in agreement with the UL obtained in the O3 isotropic search.

Phenomenological model parameters and energy density spectrum for BC and SW

The parameters to consider are the following:

- $T_{\rm pt}$: temperature after the GW generation (GeV).
- v_w: bubble wall 'terminal' velocity (units of speed of light).
- α : strength of the transition.
- $\frac{\beta}{H_{\rm pt}}$, with β the inverse duration of the FOPT ($H_{\rm pt}$=hubble rate at the time of the transition).
- $\kappa_t, \kappa_\phi, \kappa_{sw}$: 'efficiencies' of each type of signal.

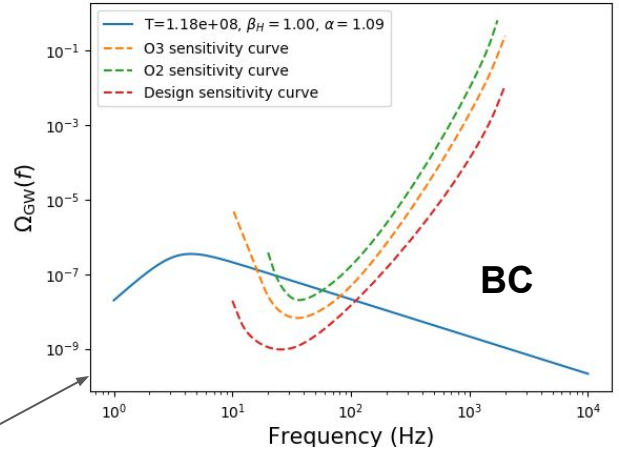

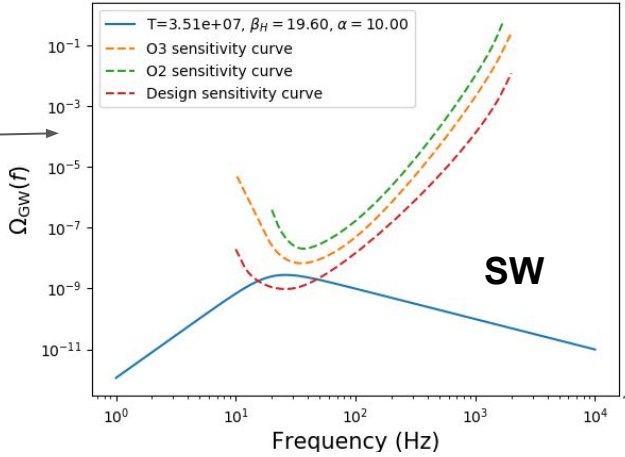

The red curve is the O3 sensitivity (that with respect to which we have compared our models). The orange curve is the sensitivity expected for Ad-LIGO +.

Priors and results from the CBC+phenomelogical model for FOPTs (BC) search

We use the energy density spectrum given by Eqs. (1) and (3) from Phys. Rev. Lett. 126, 151301 – Published 16 April 2021.

Phenomenological model	
Parameter	Prior
$\Omega_{\rm ref}$	LogUniform(10^{-10}, 10^{-7})
α	LogUniform (10^{-3}, 10)
$\beta/H_{\rm pt}$	LogUniform (10^{-1}, 10^{3})
$T_{\rm pt}$	LogUniform (10^{5}, 10^{10} GeV)
$v_{\rm w}$	1
κ_{ϕ}	1
$\kappa_{\rm sw}$	$f(\alpha, v_{\rm w}) \in [0.1 - 0.9]$

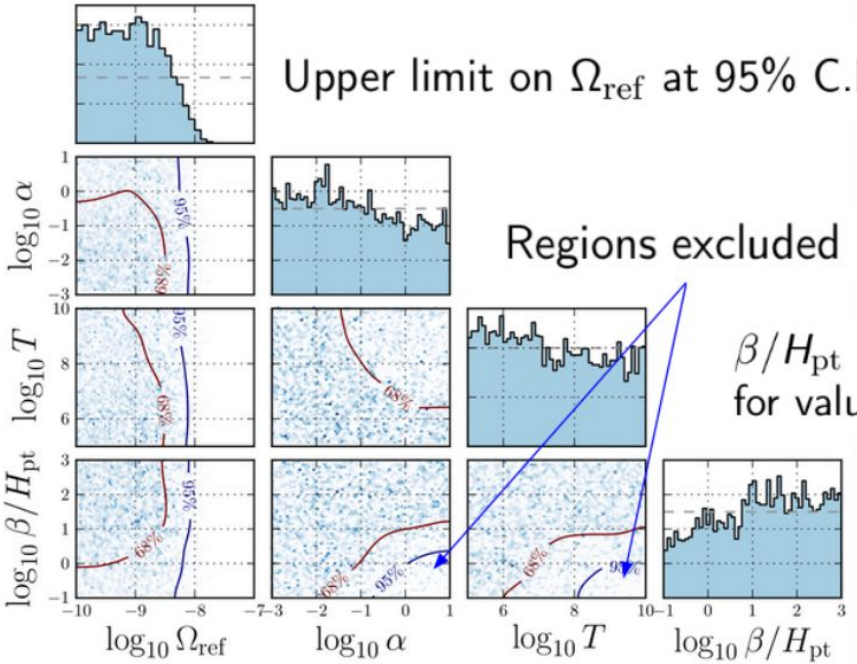

In the case of SW sourcing the generation of GWs, we cannot make exclusions in parameter space except for the amplitude of the CBC background (UL at 95% CL of 5.86×10^{-9}

PBHs

PBHs formation

- PBHs were formed in the early radiation-dominated era.
- Source: highly over-dense region that would gravitationally collapse into a black hole, known as primordial (PBH). Said otherwise, PBHs are the product of the collapse of large density perturbations ($\delta \sim 0.01$, where δ denotes the density contrast of the patch).

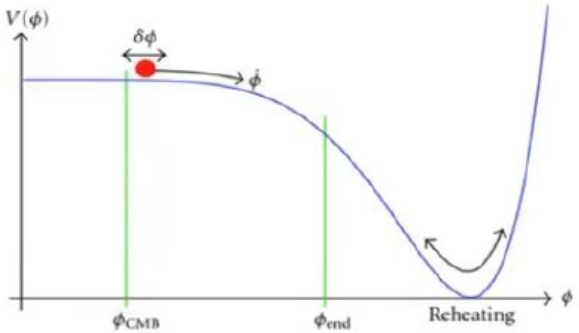

- These density perturbations could have been formed during inflation (due to quantum fluctuations of ϕ).
- In the case of "slow roll" inflation, the production would be from ϕ_{CMB} to ϕ_{end}.
- The collapse takes place when the large fluctuations re-enter horizon.

Production of GWs

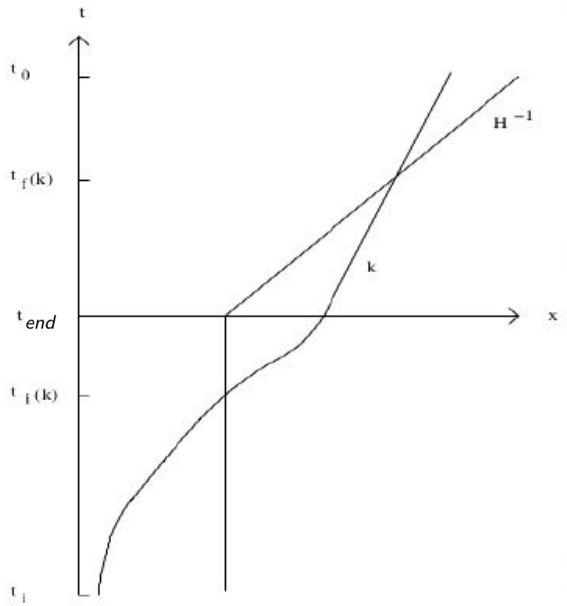

Figure 1: Scale re-entering the horizon

- Inflationary period $t \in [t_i, t_{end}]$.
- During inflation, the Hubble radius H^{-1} is constant in spatial coordinates, whereas it increases linearly in time after t_{end}.
- The physical length corresponding to a fixed comoving length scale (k) increases exponentially during inflation but increases less fast than the Hubble radius after t_{end}.
- This leads k to re-enter the horizon, which is when GWs are generated (at the same epoch as the PBH formation).

Curvature power spectrum

- We choose a log-normal shape to describe the peak in the curvature power spectrum (this is just a choice of parametrisation).

$$\mathcal{P}_\zeta(k) = \frac{A}{\sqrt{2\pi}\Delta} \exp\left[-\frac{\ln^2(k/k_*)}{2\Delta^2}\right]$$

- A is the integrated power of the peak.
- Δ determines the width of the peak.
- k_* is the position of the peak. It is more common to use k than f, and they are related by:

$$f_*/\mathrm{Hz} = 1.6\times10^{-15} k_*/\mathrm{Mpc}^{-1}$$

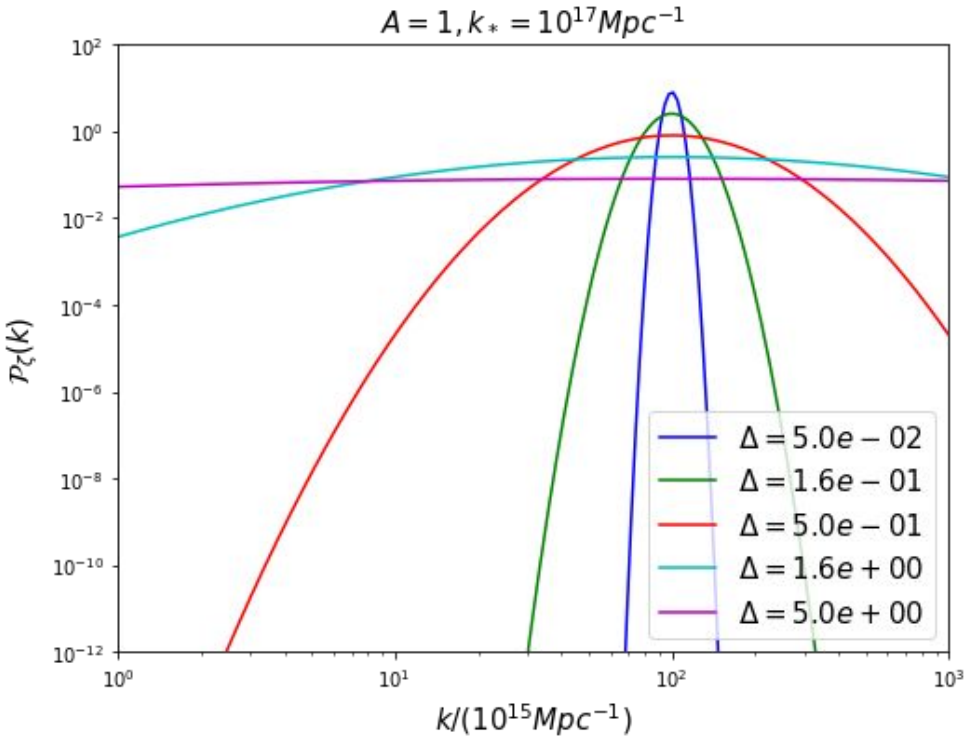

The SIGW spectrum

Spectrum for scalar induced gravitational waves (SIGW): [1]

$$\Omega_{GW}(f) = 0.387 \cdot \Omega_R \left(\frac{g_{*,s}^4 g_*^{-3}}{106.75}\right)^{-1/3} \frac{1}{6} \int_{-1}^{1} dx \int_{1}^{\infty} dy \mathcal{P}\left(\frac{y-x}{2} f\right) \mathcal{P}\left(\frac{x+y}{2} f\right) F(x,y)$$

~100 (scales larger than 10^{15} Mpc^{-1} reentered the horizon at T>10^{8} GeV)

5.38e-5

- At Δ<<1 the amplitude of the induced GWs as well as the generated PBH abundance are independent on Δ, whereas for Δ>1 they are determined by . $\mathcal{P}_\zeta(k_*) = A/(\sqrt{2\pi}\Delta)$
- This spectrum is peaked around the same wavenumber as the curvature power spectrum and its peak amplitude is $\Omega_{\rm GW} = \mathcal{O}(10^{-5})A^2$ for $\Delta \ll 1$

[1] K. Kohri and T. Terada, Phys. Rev. D97, 123532(2018), 1804.08577

The SIGW spectrum

- The LIGO-Virgo detectors, being sensitive to frequencies between 10-500Hz, can potentially probe peaks in the curvature power spectrum at scales (k) larger than 10^{15} Mpc^{-1} and smaller than 10^{18} Mpc^{-1}.
- CMB observations show that at large scales the amplitude of the curvature power spectrum is of the order of 10^{-9} → SIGW cannot be probed.
- For PBHs to form, the curvature power spectrum amplitude needs to be of the order of 0.01 at small scales → SIGW within the reach of GW observatories.

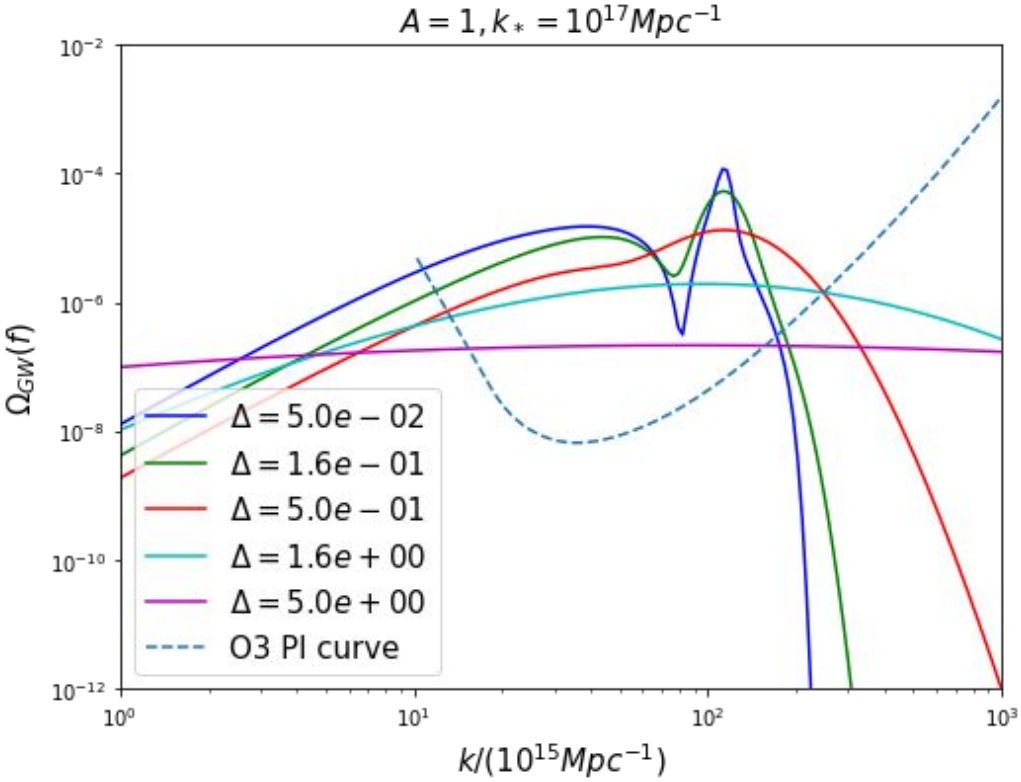

Priors used in the Bayesian search

- To the SIWG, as we mentioned before, we add the non-negligible contribution from CBCs, which we model as a simple power law with f_{ref}=25Hz:

$$\Omega_{\rm CBC} = \Omega_{\rm ref} (f/f_{\rm ref})^{2/3}$$

- We then chose the priors in the table to the right, where A and k_* are chosen so that the resulting peak in the GW spectrum is comparable with the LIGO-Virgo sensitivity. The prior on Δ is chosen so that the range covers both very narrow and broad spectra. Finally, the prior on $\Omega_{\rm ref}$ comes from previous estimates of the CBC background [3,4].

Parameter	Prior
$\Omega_{\rm ref}$	$\mathrm{LogUniform}(10^{-10}, 10^{-7})$
A	$\mathrm{LogUniform}(10^{-3}, 10^{0.5})$
k_*/Mpc^{-1}	$\mathrm{LogUniform}(10^{13}, 10^{21})$
Δ	$\mathrm{LogUniform}(0.05, 5)$

[3] R. Abbott et al. (LIGO Scientific, Virgo, KAGRA) (2021), 2101.12130.

[4] B. P. Abbott et al. (LIGO Scientific, Virgo), Phys. Rev. Lett. 120, 091101 (2018), 1710.05837.

Results from the Bayesian search

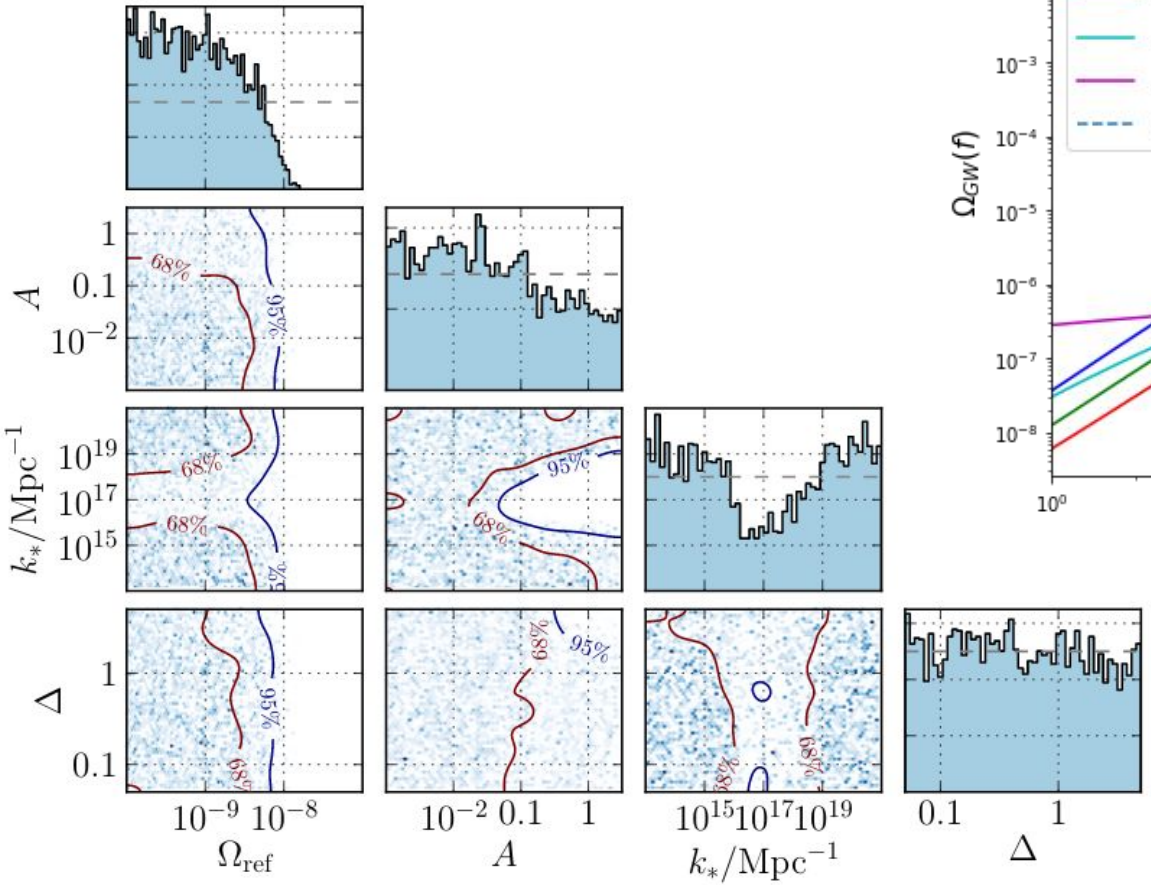

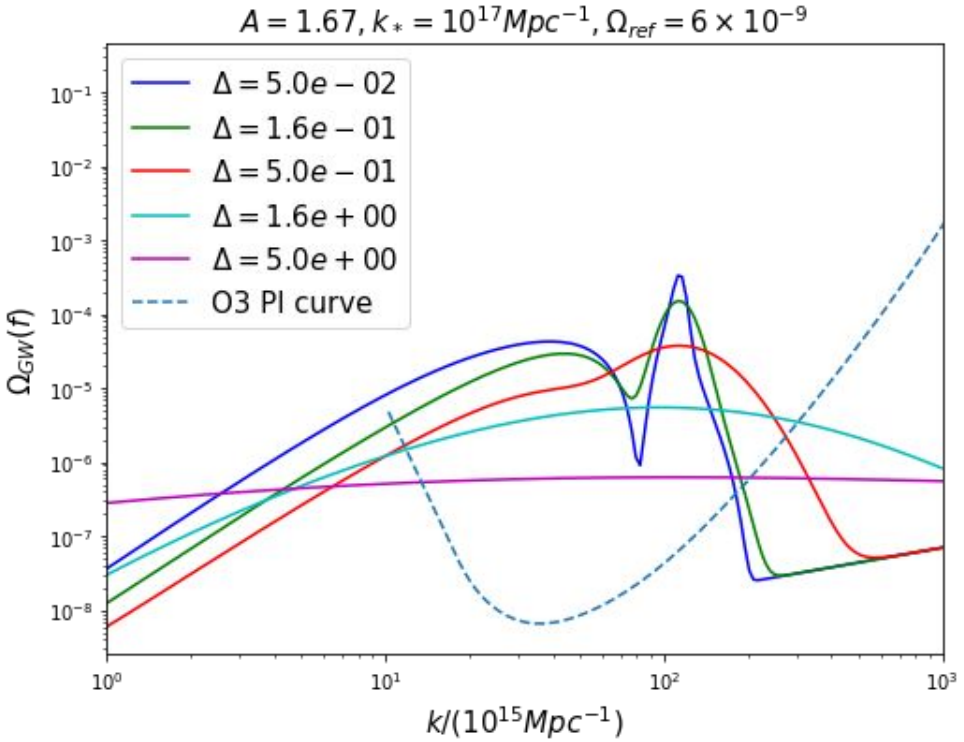

- UL at 95 CL on Omega_CBC: 6.02e-09
- UL at 95 CL on A: 1.67e+00
- Log Bayes factor of signal vs noise: -0.8

UL at 95% CL on A

- We run 12 more searches where we set delta priors over k_* and Δ to obtain upper limits at 95 % CL on the integrated power A of the peak in the curvature power spectrum:

	$k_* = 10^{15}\,\mathrm{Mpc}^{-1}$	$k_* = 10^{17}\,\mathrm{Mpc}^{-1}$	$k_* = 10^{19}\,\mathrm{Mpc}^{-1}$
$\Delta = 0.05$	2.1	0.02	1.4
$\Delta = 0.2$	2.2	0.03	1.6
$\Delta = 1$	1.6	0.05	1.8
$\Delta = 5$	0.2	0.2	0.3

- For Δ>1, the ULs on A do not depend on the peak position (k_*), whereas for Δ<1, the most stringent bound on A is obtained at the peak frequency near the best sensitivity of LIGO-Virgo detectors. The strongest exclusion, A < 0.02, is obtained for a narrow peak at $k_* = 10^{17}$ Mpc^{-1}.
- In all of these searches, the UL at 95% CL on Ω_{ref} is between 5.5e-9 to 6.6e-9, which is in agreement with the UL obtained in the O3 isotropic search.

$\Omega_{GW}(f)$ from the contribution of CBCs + PBHs, for fixed f_* and Δ

Increasing k_*

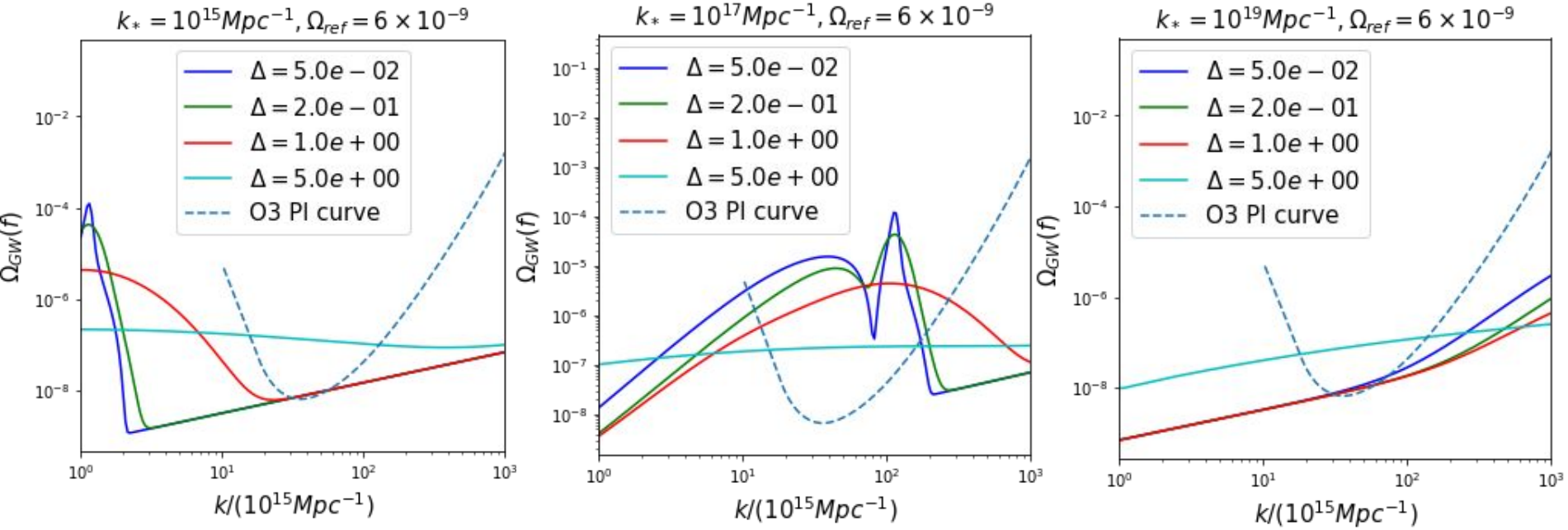

As seen in the previous slide, the most stringent ULs are obtained for $k_* = 10^{17}$ Mpc^{-1}, and for large Δ, the spectrum is independent of k_*.

Implications for PBHs

- We compare constraints arising from BBN/CMB and PBH formation with the 95% CL LIGO-Virgo bound for A as a function of k $*$ obtained from our Bayesian analysis.
- We show the LIGO-Virgo bounds from running two searches with these curvature power spectrum:
  - Dirac delta function peak ($\Delta \to 0$)
  - Log-normal peak with $\Delta = 1$
- We calculate the PBH abundance generated from the peak in the curvature power spectrum shown earlier,

$$\mathcal{P}_\zeta(k) = \frac{A}{\sqrt{2\pi}\Delta} \exp\left[-\frac{\ln^2(k/k_*)}{2\Delta^2}\right]$$

and then follow the procedure in [5]. We also use: $M_{\rm PBH} \sim M_k$ to show the PBH mass associated to certain k.

---

[5] S. Young, I. Musco, and C. T. Byrnes, JCAP 11, 012 (2019), 1904.00984.

- In the range of k_* from 10^{15}-10^{18} Mpc^{-1} the LIGO-Virgo bound is stronger than the indirect bounds on the abundance of GWs arising from BBN, $\Omega_{GW} < 3.7 \times 10^{-6}$ and the CMB observations, $\Omega_{GW} < 3.5 \times 10^{-6}$.
- The relevant PBH masses for our sensitivity band are $M_{\rm PBH} \lesssim 10^{16}\,{\rm g}$.
- Our current LIGO-Virgo sensitivity is not enough to constrain the PBH formation.

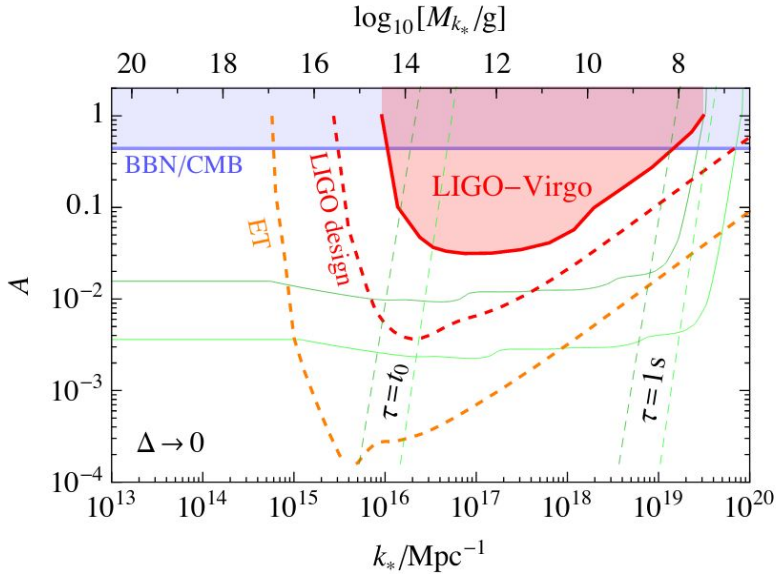

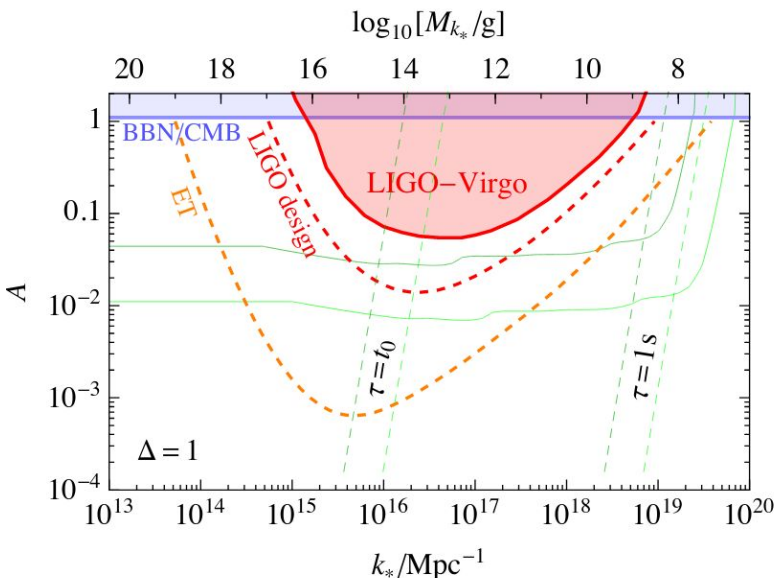

The dashed red and orange curves show the projected sensitivities of LIGO in its final phase and ET. The green dashed curves indicate the evaporation timescales of the PBHs.

Conclusions

- We recast the results from the isotropic SGWB searches in terms of constraints to FOPT and PBH inspired models.
- We used the LIGO-Virgo O1+O2+O3 correlated data and were able to place upper limits over the parameters of our models with a Bayesian formalism.
- In the case that the SGWB is sourced by:
    - CBCs+FOPTs: for $T_{\rm pt} \in [10^7, 10^9]$ GeV the produced SGWB is within the frequency range of Ad-LIGO and AdV $\rightarrow$ we have excluded regions in parameter space at 95% CL. These results indicate the relevance of the LIGO-Virgo GW data to place constraints on new phenomena related to strong FOPTs at large T in the early Universe.
    - CBCs+PBHs: we showed that the obtained constraints are stronger than the ones arising from BBN and CMB observations in the range of scales from 10^{15}-10^{18} Mpc^{-1}. The tightest constraints (for a narrow peak at $k_* = 10^{17}$ Mpc^{-1}) are less stringent than those arising from the abundance of PBHs that such peak in the curvature power spectrum corresponds to.
- However, we find that current ground-based experiments at their design performance, and the future Einstein Telescope will reach the required sensitivity.